J|A|C|S
ARTICLES
Published on Web 01/06/2006

Optimization of the Molecular Orbital Energies of Conjugated Polymers for Optical Amplification of Fluorescent Sensors

Bin Liu and Guillermo C. Bazan*

Contribution from the Department of Materials and Chemistry and Biochemistry, Institute for Polymers and Organic Solids, University of California at Santa Barbara, Santa Barbara, California 93106

Received August 6, 2005; E-mail: bazan@chem.ucsb.edu

Abstract: Cationic water-soluble poly(fluorene-*co*-phenylene)s with electron withdrawing or donating substituents on the conjugated backbone were designed and synthesized. Fluorescence resonance energy transfer (FRET) experiments between these conjugated polymers and dye-labeled single-stranded DNA (ssDNA-C*) reveal the importance of matching donor and acceptor orbital energy levels to improve the sensitization of C* emission. Quenching of polymer fluorescence with ssDNA-C* and differences in C* emission suggest involvement of photoinduced charge transfer (PCT) as an energy wasting mechanism. The HOMO and LUMO energy levels of the conjugated polymers and C* serve as a preliminary basis to understand the competition between FRET and PCT. Dilution of C* in polymer/ssDNA-C* complexes by addition of ssDNA yields insight into C*···C* self-quenching. Under optimized conditions, where there is no probe self-quenching and minimum PCT, efficient signal amplification is demonstrated despite poor spectral overlap between polymer and C*.

Introduction

Conjugated polymers (CPs) form the basis of new methods for the trace detection of analytes in a variety of environments.[1,2] Their delocalized electronic structure allows for electronic coupling between optoelectronic segments and efficient intra- and interchain energy transfer.[3] Important properties, such as charge transport,[4] conductivity,[5] emission intensity,[2a,2f,2g] and exciton migration[4] are easily perturbed by external agents, leading to substantial changes in measurable signals.[6] For interrogation in aqueous media, conditions typically required for biosensor applications, one relies on CPs with charged pendant groups (i.e., conjugated polyelectrolytes).[2,7] These water soluble CPs have been used as light harvesting molecules that deliver excitations to signaling fluorescent dyes attached to biomolecular probes, thereby providing increased signal intensities and sensitivities above those of single molecule reporters.[6,8] Nonspecific contacts between nontarget species and the hydrophobic CP backbone need special attention for attaining selectivity, as these interactions can lead to misleading interpretations of results.[9]

(1) (a) Yang, J. S.; Swager, T. M. *J. Am. Chem. Soc.* **1998**, *120*, 11864. (b) Yang, J. S.; Swager, T. M. *J. Am. Chem. Soc.* **1998**, *120*, 5321. (c) Leclerc, M. *Adv. Mater.* **1999**, *11*, 1491. (d) McQuade, D. T.; Pullen, A. E.; Swager, T. M. *Chem. Rev.* **2000**, *100*, 2537. (e) Ewbank, P. C.; Nuding, G.; Suenaga, H.; McCullough, R. D.; Shinkai, S. *Tetrahedron Lett.* **2001**, *42*, 155. (f) Ho, H. A.; Boissinot, M.; Bergeron, M. G.; Corbeil, G.; Doré, K.; Boudreau, D.; Leclerc, M. *Angew. Chem.* **2002**, *41*, 1548. (g) Kim, I. B.; Erdogan, B.; Wilson, J. N.; Bunz, U. H. F. *Eur. J. Chem.* **2004**, *10*, 6247. (h) Rose, A; Zhu, Z. G.; Madigan, C. F.; Swager, T. M.; Bulovic, V. *Nature* **2005**, *434*, 876. (i) Kim, I. B.; Dunkhorst, A.; Gilbert, J.; Bunz, U. H. F. *Macromolecules*, **2005**, *38*, 4560. (j) Kim, I. B.; Wilson, J. N.; Bunz, U. H. F. *Chem. Commun.* **2005**, *10*, 1273.

(2) (a) Chen, L.; McBranch, D. W.; Wang, H.; Helgeson, R.; Wudl, F.; Whitten, D. *Proc. Natl. Acad. Sci. U.S.A.* **1999**, *96*, 12287. (b) DiCesare, N.; Pinto, M. R.; Schanze, K. S.; Lakowicz, J. R. *Langmuir* **2002**, *18*, 7785. (c) Liu, B.; Bazan, G. C. *Chem. Mater.* **2004**, *16*, 4467. (d) Leclerc, M.; Ho, H. A. *Synlett* **2004**, *2*, 380. (e) Disney, M. D.; Zheng, J.; Swager, T. M.; Seeberger, P. H. *J. Am. Chem. Soc.* **2004**, *126*, 13343. (f) Kumaraswamy, S.; Bergstedt, T.; Shi, X.; Rininsland, F.; Kushon, S.; Xia, W. S.; Ley, K.; Achyuthan, K.; McBranch, D.; Whitten, D. *Proc. Natl. Acad. Sci. U.S.A.* **2004**, *101*, 7511. (g) Pinto, M. R.; Schanze, K. S. *Proc. Natl. Acad. Sci. U.S.A.* **2004**, *101*, 7505. (h) Le Floch, F.; Ho, H. A.; Harding, L. P.; Bedard, M.; Neagu, P. R.; Leclerc, M. *Adv. Mater.* **2005**, *17*, 1251. (i) Ho, H. A.; Bers-Aberem, M.; Leclerc, M. *Eur. J. Chem.* **2005**, *11*, 1718. (j) Wosnick, J. H.; Mello, C. M.; Swager, T. M. *J. Am. Chem. Soc.* **2005**, *127*, 3400. (k) Nilsson, K. P. R.; Inganäs, O. *Nat. Mater.* **2003**, *2*, 419. (l) Nilsson, K. P. R.; Olsson, J. D. M.; Stabo-Eeg, F.; Lindgren, M.; Konradsson, P.; Inganäs, O. *Macromolecules* **2005**, *38*, 6813. (m) Herland, A.; Nilsson, K. P. R.; Olsson, J. D. M.; Hammarstrom, P.; Konradsson, P.; Inganäs, O. *J. Am. Chem. Soc.* **2005**, *127*, 2317.

(3) (a) Guillet, J. E. *Polymer Photophysics and Photochemistry*; Cambridge University Press: Cambridge, 1985. (b) Weber, S. E. *Chem. Rev.* **1990**, *90*, 1469. (c) Kauffmann, H. F. *Photochemistry and Photophysics*; Radek, J. E., Ed.; CRC: Boca Raton, FL, 1990; Vol 2. (d) Scholes, G. D.; Ghiggino, K. P. *J. Chem. Phys.* **1994**, *101*, 1251. (e) Tasch, S.; List, E. J. W.; Hochfilzer, C.; Leising, G.; Schlichting, P.; Rohr, U.; Geerts, Y.; Scherf, U.; Mullen, K. *Phys. Rev. B* **1997**, *56*, 4479. (f) Nguyen, T. Q.; Wu, J. J.; Doan, V.; Schwartz, B. J.; Tolbert, S. H. *Science* **2000**, *288*, 652. (g) Pschirer, N. G.; Byrd, K.; Bunz, U. H. F. *Macromolecules* **2001**, *34*, 8590. (h) Beljonne, D.; Pourtois, G.; Silva, C.; Hennebicq, E.; Herz, L. M.; Friend, R. H.; Scholes, G. D.; Setayesh, S.; Müllen, K.; Brédas, J. L. *Proc. Natl. Acad. Sci. U.S.A.* **2002**, *99*, 10982. (i) Liu, B.; Wang, S.; Bazan, G. C.; Mikhailovsky, A. *J. Am. Chem. Soc.* **2003**, *125*, 13306. (j) Liu, B.; Bazan, G. C. *J. Am. Chem. Soc.* **2004**, *126*, 1942. (k) Hennebicq, E.; Pourtois, G.; Scholes, G.; Herz, L.; Russell, D.; Silva, C.; Setayesh, S.; Grimsdale, A. C.; Müllen, K.; Brédas, J.; Beljonne, D. *J. Am. Chem. Soc.* **2005**, *127*, 4744.

(4) Lee, D. W.; Swager, T. M. *Synlett* **2004**, 149.

(5) (a) Korri, Y. H.; Garnier, F.; Srivastava, P.; Godillot, P.; Yassar, A. *J. Am. Chem. Soc.* **1997**, *119*, 7388. (b) Bäuerle, P.; Emge, A. *Adv. Mater.* **1998**, *10*, 324. (c) Garnier, F.; Korri, Y. H.; Srivastava, P.; Mandrand, B.; Delair, T. *Synth. Met.* **1999**, *100*, 89. (d) Korri-Y, H.; Yassar, A. *Biomacromolecules* **2001**, *2*, 58.

(6) Swager, T. M. *Acc. Chem. Res.* **1998**, *31*, 201.

(7) (a) Pinto, M. R.; Schanze, K. S. *Synthesis* **2002**, *9*, 1293. (b) Traser, S.; Wittmeyer, P.; Rehahn, M. *e-Polymers* **2002**, No. 032.

(8) (a) McQuade, D. T.; Hegedus, A. H.; Swager, T. M. *J. Am. Chem. Soc.* **2000**, *122*, 12389. (b) Gaylord, B. S.; Heeger, A. J.; Bazan, G. C. *Proc. Natl. Acad. Sci. U.S.A.* **2002**, *99*, 10954. (c) Kim, T. H.; Swager, T. M. *Angew. Chem.* **2003**, *42*, 4803. (d) Gaylord, B. S.; Heeger, A. J.; Bazan, G. C. *J. Am. Chem. Soc.* **2003**, *125*, 896.

(9) Dwight, S. J.; Gaylord, B. S.; Hong, J. W.; Bazan, G. C. *J. Am. Chem. Soc.* **2004**, *126*, 16850.

10.1021/ja055382t CCC: $33.50 **© 2006 American Chemical Society**

Scheme 1. Effect of Relative Orbital Energy Levels on FRET versus PCT Preferences

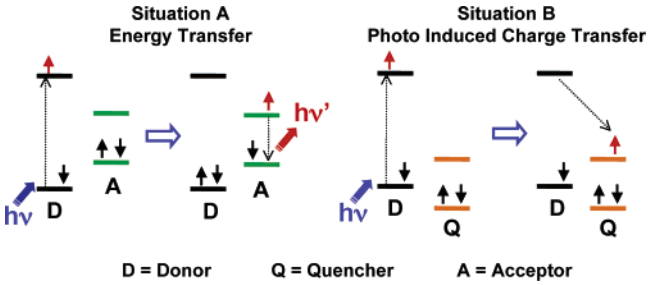

One specific approach that improves the sensitivity of fluorescent DNA assays involves using a cationic conjugated polymer (CCP) and a chromophore labeled DNA (DNA-C*), which are selected to favor fluorescence resonance energy transfer (FRET) from the CCP to the DNA-C*.[2c,8d] Amplification of C* emission by excitation of CCPs, relative to direct excitation of C*, originates from the polymer's large absorption cross-section. Efficient CCP to C* FRET is a required additional condition to increase sensitivity.[10] Eq 1 describes how the FRET rate (k_t) changes as a function of the donor−acceptor distance (r), the orientation factor (κ), and the overlap integral (J), where $F_D(\lambda)$ is the corrected fluorescence intensity of the donor in the range of λ to $\lambda + \Delta\lambda$ and $\epsilon_A(\lambda)$ is the extinction coefficient of the acceptor at λ.[11]

$$k_t \propto \frac{1}{r^6}\kappa^2 J(\lambda) \qquad (1)$$

$$J(\lambda) = \int_0^\infty F_D(\lambda)\epsilon_A(\lambda)\lambda^4 d\lambda$$

According to eq 1, maximized overlap ($J(\lambda)$) between the emission of the CCP and the absorption of C* should provide for optimum FRET conditions.

Recent studies of conjugated phenylenevinylene-based dendrimers and binary conjugated polymer blends highlight the competition between energy transfer and photoinduced charge transfer (PCT) events as a function of the HOMO and LUMO energy levels in the donor and acceptor pairs.[12] Scheme 1 provides a simplified illustration of two situations that may occur upon donor excitation.[13] Situation A corresponds to the ideal situation for FRET, where the HOMO and LUMO energy levels of the acceptor are located within the orbital energy levels of the donor. Upon excitation of the donor, energy transfer from the donor to the acceptor takes place, leading to an emissive process, provided that the emission quantum yield of the acceptor is sufficiently large. There is no quenching of the acceptor under Situation A.

When the energy levels of the acceptor are not contained within the orbital energies of the donor, in other words, when both the electron affinity and the ionization potential are higher in one of the optical partners, as in situation B, donor excitation may lead to photoinduced charge transfer.[14] As shown in Scheme 1, donor excitation would lead to photoinduced electron transfer to the acceptor. Excitation of the acceptor would lead to a similar charge separated state via hole transfer to the donor.[13] While Scheme 1 is widely used for choosing suitable optical partners for a specific application, it fails to be accurate for intermediate cases since it neglects contributions from the exciton binding energy, the intermolecular charge transfer state energy, and the stabilization of the charged species by the medium.[14d] The mechanism by which FRET or PCT is preferred is complex for conjugated polymer blends and may involve geminate electron−hole pairs that convert to exciplexes and ultimately excitons.[15] Despite these uncertainties, Scheme 1B provides for a necessary, but not sufficient, condition for PCT.

Scheme 2. Major Interactions within CCP/DNA-C* Complexes that Influence Optical Performance

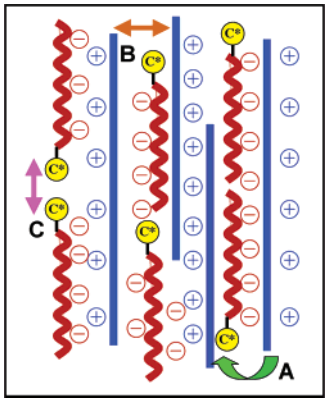

Electrostatic interactions between CCPs and phosphate groups in DNA bring CCPs and DNA-C* into close proximity to satisfy the FRET distance requirement. Hydrophobic interactions are also operative; however, these are less well understood and may be controlled to some extent by solvent choice.[16] CCP/DNA-C* complexes are dynamic structures of varying sizes. Three major types of interactions that influence optical performance within these structures can be readily identified (shown in Scheme 2): CCP···C* (A), CCP···CCP (B), and C*···C* (C). Close association between CCP and DNA-C* will favor FRET, while close contact among C* units may cause self-quenching, ultimately leading to decreased signal amplification. Interchain contacts (CCP···CCP) can also lead to donor self-quenching and a reduction of fluorescence amplification. Despite the general success of using CCPs in biosensor schemes,[3i,3j,8d,16b,17] there is little information available on how the geometry, size, and orientation between optical partners in these kinetically formed CCP/DNA-C* structures influence optical output.[18]

(10) Förster, T. *Ann. Phys.* **1948**, *2*, 55.
(11) Lakowicz, J. R. *Principles of Fluorescence Spectroscopy*; Kluwer Academic/Plenum Publisher: New York, 1999.
(12) (a) Halls, J. J. M.; Cornil, J.; Santos, D. A.; Silbey, R.; Hwang, D. H.; Holmes, A. B.; Brédas, J. L.; Friend, R. H. *Phys. Rev. B* **1999**, *60*, 5721. (b) Segura, J. L.; Gómez, R.; Martín, N.; Luo, C.; Swartz, A.; Guldi, D. M. *Chem. Commun.* **2001**, *8*, 707. (c) Guldi, D. M.; Swartz, A.; Luo, C.; Gómez, R.; Segura, J.; Martín, N. *J. Am. Chem. Soc.* **2002**, *124*, 10875.
(13) Cornil, J.; Lemaur, V.; Steel, M. C.; Dupin, H.; Burquel, A.; Beljonne, D.; Bredas, J. L. In *Organic Photovoltaics*; Sun, S. J., Sariciftci, N. S., Eds.; Taylor and Francis: Boca Raton, FL, 2005; p 161.
(14) (a) Sariciftci, N. S.; Smilowitz, L.; Heeger, A. J.; Wudl, F. *Science* **1992**, *258*, 1474. (b) Marcus, R. A. *Angew. Chem. Int. Eng.* **1993**, *32*, 1111. (c) Xu, Q. H.; Moses, D.; Heeger, A. J. *Phys. Rev. B* **2003**, *67*, 245417. (d) Brédas, J. L.; Beljonne, D.; Coropceanu, V.; Cornil, J. *Chem. Rev.* **2004**, *104*, 4971. (e) Thomas, K. R. J.; Thompson, A. L.; Sivakumar, A. V.; Bardeen, A. J.; Thayumanavan, S. *J. Am. Chem. Soc.* **2005**, *127*, 373.
(15) Morteani, A. C.; Sreearunothai, P.; Herz, L. M.; Friend, R. H.; Silva, C. *Phys. Rev. Lett.* **2004**, *92*, 247402.
(16) (a) Ganachaud, F.; Elaissari, A.; Pichot, C.; Laayoun, A.; Cros, P. *Langmuir* **1997**, *13*, 701. (b) Liu, B.; Gaylord, B. S.; Wang, S.; Bazan, G. C. *J. Am. Chem. Soc.* **2003**, *125*, 6705.
(17) (a) Wang, S.; Gaylord, B. S.; Bazan, G. C. *Adv. Mater.* **2004**, *16*, 2127. (b) Gaylord, B. S.; Massie, M. R.; Feinstein, S. C. *Proc. Natl. Acad. Sci. U.S.A.* **2005**, *102*, 34. (c) Xu, H.; Wu, H. P.; Huang, F.; Song, S. P.; Li, W. X.; Cao, Y.; Fan C. H. *Nucleic Acids Res.* **2005**, *33*, e83.

Scheme 3. Synthesis of CCPs **1**, **2**, and **3**[a]

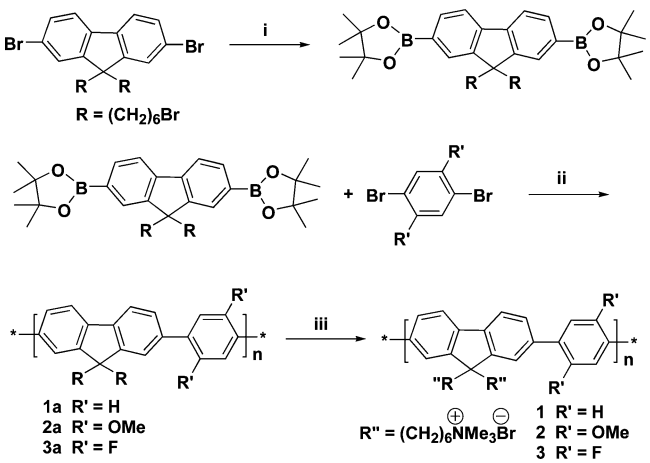

[a] Reaction conditions: (i) *t*-BuLi/pentane, 2-isopropoxy-4,4,5,5-tetramethyl-1,3,2-dioxaborolane, THF, −78 °C, 3 h; (ii) $Pd(PPh_3)_4$, 2 M Na_2CO_3, toluene; and (iii) NMe_3, THF/H_2O.

In this contribution, we probe the importance of matching the energy levels between CCPs and C* for determining C* emission and FRET efficiency. We begin by examining the optical and electronic properties of three specifically designed CCP structures and the FRET from the CCPs to fluorescein- (Fl) or Texas Red- (TR) labeled ssDNA. We then report studies on CCP self-quenching with unlabeled ssDNA and on C* emission quenching upon CCP/DNA-C* complex formation. The HOMO and LUMO energy levels of the CCPs and C* serve as a basis for understanding the competition between energy transfer and PCT processes from a thermodynamics perspective. Finally, we show how this information is useful to control ssDNA-TR/polymer interactions and to improve signal amplification.

Results

Synthesis. Scheme 3 shows the synthetic route to the CCP structures used in this study. The sequence of steps circumvents time-consuming protection−deprotection steps or tedious purification procedures associated with amine-containing intermediates.[19] The key intermediate, 2,7-bis[9,9′-bis(6″-bromohexyl)-fluorenyl]-4,4,5,5-tetramethyl-[1.3.2]dioxaborolane was synthesized in one step, starting from 2,7-dibromo-9,9′-bis(6″-bromohexyl)fluorene.[16b] After the addition of *t*-BuLi, excess 2-isopropoxy-4,4,5,5-tetramethyl-1,3,2-dioxaborolane was added in a single portion to the reaction mixture, and the reaction was continued for another 2 h. It is necessary to keep the reaction temperature at −78 °C to minimize nucleophilic reaction between the aliphatic bromide at the fluorene 9-position and the lithium salt byproduct. The boronic ester was purified by chromatography using silica support, and the molecular structure was confirmed by MS and NMR spectroscopies. The availability of the alkylbromide-containing arylboronates greatly simplifies the synthesis of water-soluble conjugated polymer precursors that rely on Suzuki cross-coupling protocols.

Table 1. Summary of Absorption and PL Spectra in 25 mM Phosphate Buffer (pH = 7.4)

compounds	$\lambda_{max\ abs.}$ (nm)	$\lambda_{max\ em.}$ (nm)	ϵ (cm^{-1} L mol^{-1}) × 10^4	Φ[a] (%)
1	385	415	4.54	24
2	363	410	4.05	32
3	369	414	4.18	29
Fl	495	515	7.50	85
TR	590	615	8.30	90[b]

[a] Using quinine sulfate as the standard, ±5% error.[22] [b] Molecular Probes (http://probes.invitrogen.com).

Scheme 4. Chemical Structures of Fl and TR with Linkers (8-Amino-3,6-dioxaoctanoic Acid) Prior to ssDNA Attachment

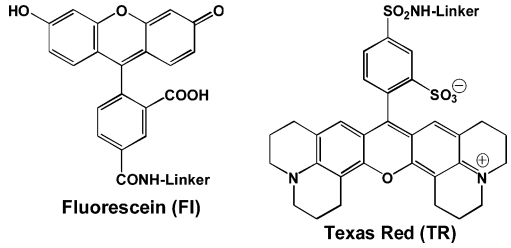

Poly[9,9′-bis(6″-(*N*,*N*,*N*-trimethylammonium)-hexyl)fluorene-*co*-*alt*-1,4-phenylene dibromide] (**1**),[3i] poly[9,9′-bis(6″-(*N*,*N*,*N*-trimethylammonium)-hexyl)fluorene-*co*-*alt*-2,5-dimethoxy-1,4-phenylene dibromide] (**2**), and poly[9,9′-bis(6″-(*N*,*N*,*N*-trimethylammonium)-hexyl)fluorene-*co*-*alt*-2,5-difluoro-1,4-phenylene dibromide] (**3**) were synthesized via Suzuki coupling under refluxing conditions in a mixture of 2 M Na_2CO_3/toluene with $Pd(PPh_3)_4$ as the catalyst,[20] followed by trimethylamine treatment (Scheme 3). Suzuki copolymerization of 2,7-bis[9,9′-bis-(6″-bromohexyl)-fluorenyl]-4,4,5,5-tetramethyl-[1.3.2]dioxaborolane and 1,4-dibromobenzene derivatives provides the neutral polymer precursors **1a**, **2a**, and **3a** in 73−78% yields. Formation of the ionic water-soluble polymers **1**−**3** was achieved in 83−89% yields via quaternization of the neutral polymers with trimethylamine in a THF/water mixture. ^1H and ^{13}C NMR spectroscopies confirm the molecular structures in Scheme 3. The degree of quaternization is greater than 90%, as calculated from the ratio of the integrated areas for $C\underline{H}_2CH_2X$ (X = Br, $N(CH_3)_3$) and $CH_2CH_2N(C\underline{H}_3)_3$ in the ^1H NMR spectra. GPC determined molecular weights (M_n) are 27 000 (PDI = 2.2), 35 000 (PDI = 2.0), and 28 000 (PDI = 1.5) for **1**−**3**, respectively.

Optical and Electronic Properties. Table 1 summarizes of the absorption and photoluminescence (PL) spectra of **1**−**3**, Fl, and TR (structures shown in Scheme 4). Figure 1 shows the PL spectra of **1**−**3** and the absorption of Fl and TR attached to the 5′-position of ssDNA-C* (sequence: 5′-C*-ATC TTG ACT ATG TGG GTG CT-3′, C* = Fl or TR). Measurements were made in 25 mmol phosphate buffer at pH = 7.4, conditions typically used in DNA detection schemes. For **1**, the absorption maximum (λ_{abs}) appears at 385 nm and the emission maximum (λ_{em}) at 415 nm. The absorption maxima of **2** and **3** are slightly blue shifted relative to that of **1**, probably as a result of steric interference, which prevents an equally coplanar arrangement between aromatic units and thus yields less effective π-conjuga-

(18) (a) Wang, S.; Bazan, G. C. *Chem. Commun.* **2004**, *21*, 2508. (b) Wang, S.; Gaylord, B. S.; Bazan, G. C. *J. Am. Chem. Soc.* **2004**, *126*, 5446. (c) Tan, C. Y.; Pinto, M. R.; Kose, M. E.; Ghiviga, I.; Schanze, K. S. *Adv. Mater.* **2004**, *16*, 1208.
(19) (a) Stork, M.; Gaylord, B. S.; Heeger, A. J.; Bazan, G. C. *Adv. Mater.* **2002**, *14*, 361. (b) Wang, S.; Liu, B.; Gaylord, B. S.; Bazan, G. C. *Adv. Funct. Mater.* **2003**, *13*, 463.
(20) (a) Suzuki, A. *J. Organomet. Chem.* **1999**, *576*, 147. (b) Liu, B.; Bazan, G. C. In *Organic Electroluminescence*; Kafafi, Z. H., Ed.; Taylor and Francis: Boca Raton, FL, 2005; p 179. (c) Liu, B.; Yu, W. L.; Lai, Y. H.; Huang, W. *Chem. Commun.* **2000**, *7*, 551. (d) Liu, B.; Yu, W. L.; Lai, Y. H.; Huang, W. *Chem. Mater.* **2001**, *13*, 1984. (e) Liu, B.; Yu, W. L.; Lai, Y. H.; Huang, W. *Macromolecules* **2002**, *35*, 4975.

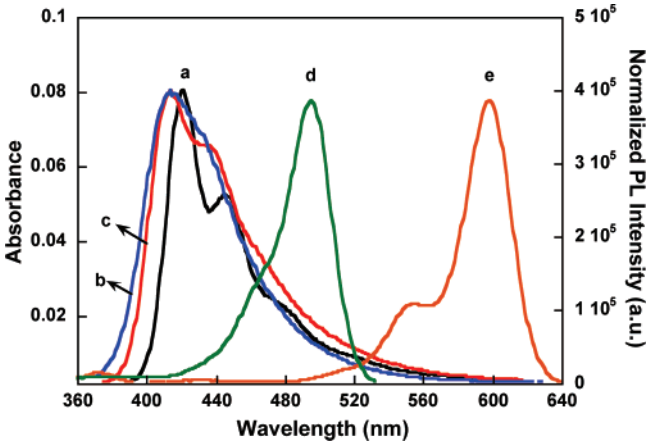

Figure 1. Photoluminescence (PL) spectra of **1** (a), **2** (b), and **3** (c) and absorbance of ssDNA-C* (Fl, d and TR, e) in 25 mM phosphate buffer (pH = 7.4). Excitation wavelength is 385 nm for **1** and 365 nm for **2** and **3**.

Table 2. Optical Bandgap and HOMO and LUMO Energies of the Neutral Precursors of **1**, **2**, **3**, Fl, and TR[a]

compound	band gap (eV)	HOMO (eV)	LUMO (eV)
1a	2.80	−5.6	−2.8
2a	2.80	−5.4	−2.6
3a	3.05	−5.8	−2.7
FL	2.30	−5.9	−3.6
TR[26]	2.08	−5.4	−3.3

[a] Cyclic voltammetry data were collected in THF or DMF using 0.1 M Bu_4NPF_6 as the electrolyte at a scan rate of 100 mV/s with a glass carbon electrode (1.6 mm diameter) as the working electrode, Pt wire as the auxiliary electrode, and $Ag/AgNO_3$ as the reference electrode.

tion.[21] However, the three CCPs show similar λ_{em}, PL band shape (Figure 1), and PL quantum yields (**1**, 24%; **2**, 32%; and **3,** 29% within ±5% error). The spectral overlap ($J(\lambda)$) between the three CCPs and the fluorescent dyes is thus similar.

The HOMO energy levels of the CCPs were estimated from the oxidation potentials of the neutral precursors determined by cyclic voltammetry (CV) in THF (Table 2).[23] Direct measurement of the oxidation and reduction potentials of CCPs in water was not successful. The corresponding LUMO levels were obtained by taking into consideration the optical bandgap from the absorption spectra. The oxidation potential onset for **1a** is 1.2 V versus SCE.[24] Introduction of the fluorine atoms on the central core increases the oxidation potential by approximately 0.2 V, while the methoxy groups lower the oxidation potential by approximately 0.2 V. In DMF, Fl displays a reversible reduction peak, with an onset reduction potential at −0.84 V versus SCE. This result is close to previous work with 5-carboxyfluorescein (−0.47 V vs NHE; NHE is −0.2412 V vs SCE[25]).[26] The first reduction potential of TR was previously reported as −0.88 V versus NHE.[27] Taking into account the optical bandgap of 2.08 eV, one obtains TR HOMO and LUMO energies of −5.36 and −3.28 eV, respectively.

FRET Measurements. We now examine how the CCP substituents influence the FRET to ssDNA-Fl by monitoring the dye emission intensity upon CCP excitation. Measurements were carried out in buffer (25 mM phosphate buffer, pH = 7.4), at a fixed ssDNA-Fl concentration (2×10^{-8} M based on strands), with [RU] varying from 0 to 4×10^{-7} M (RU = polymer repeat unit), with an increase of 5×10^{-8} M upon each polymer addition. Figure 2a shows a direct comparison of Fl emission upon CCP excitation ([RU] = 4×10^{-7} M). The most intense Fl emission was observed for **3**/ssDNA-Fl, which is approximately 2-fold more intense than that observed for **1**/ssDNA-Fl and is over an order of magnitude larger than that for **2**/ssDNA-Fl. For **3**/ssDNA-Fl, the integrated Fl emission is approximately 5-fold greater than that obtained by direct excitation of Fl at its absorption maximum (495 nm) in the absence of the CCPs, while over 20-fold enhancement is observed relative to direct Fl excitation in the presence of **3**. This enhancement is indicative of the signal amplification provided by the light harvesting capabilities of the CCPs. Additionally, the CCP sensitized Fl emission is ∼10 nm red-shifted, relative to the emission upon direct Fl excitation in the absence of the CCP.

FRET experiments using ssDNA-TR as the acceptor (with an identical base sequence to ssDNA-Fl) were also performed (Figure 2b, [ssDNA-TR] = 2×10^{-8} M and [RU] = 4×10^{-7} M). The TR emission intensities are similar for **1**/ssDNA-TR and **3**/ssDNA-TR, which are approximately twice more intense than that observed with **2**/ssDNA-TR. For **3**/ssDNA-TR, the integrated TR emission through FRET is approximately twice greater than that obtained by direct excitation of TR at its absorption maximum (590 nm) in the absence of CCPs, while there is a 10-fold enhancement relative to direct excitation of TR in the presence of **3**. Of particular significance is that the TR emission with **2**/ssDNA-TR is more intense than the Fl emission with **2**/ssDNA-Fl, despite the less effective spectral overlap ($J(\lambda)$ in eq 1).

Polymer Quenching with ssDNA and ssDNA-Fl. Figure 3 shows the decrease of CCP emission intensity ([RU] = 1×10^{-6} M) when [ssDNA] or [ssDNA-Fl] (identical base sequences) is varied from 0 to 3.5×10^{-8} M. For the three CCPs, there is a decrease in PL intensity upon the addition of ssDNA, which we attribute to chain aggregation induced by the negatively charged ssDNA and the resulting interchain quenching process.[19b] At similar CCP concentrations, the fluorescence quenching of **3** is less effective than that observed with **1** and **2**. Within the conditions in Figure 3, the loss of polymer emission upon complexation/aggregation with ssDNA varies from 0 to 20% for **3** and from 0 to 40% for **1** and **2**.

When ssDNA-Fl is added to solutions containing the CCPs, one observes a more pronounced decrease in emission, relative to the measurements with ssDNA (Figure 3). Polymer absorption was also monitored to show that there is less than 10% absorbance loss upon ssDNA-Fl addition.

Acceptor Quenching Study. Changes in the intrinsic emission properties of the reporter dyes upon CCP/ssDNA-C*

(21) Berggren, M.; Inganäs, O.; Gustafsson, G.; Rasmusson, J.; Anderson, M. R.; Hjertberg, T.; Wennerström, O. *Nature* **1994**, *372*, 444.
(22) Demas, J. N.; Crosby, G. A. *J. Phys. Chem.* **1971**, *75*, 991.
(23) Gomer, R.; Tryson, G. *J. Chem. Phys.* **1977**, *66*, 4413.
(24) Mallavia, R.; Montilla, F.; Pastor, I.; Velasquez, P.; Arredondo, V.; Alvarez, A. L.; Mateo, C. R. *Macromolecules* **2005**, *38*, 3185.
(25) Bard, A. J.; Faulkner, L. R. *Electrochemical Methods*; John Wiley & Sons: New York, 1980.
(26) Torimura, M.; Kurata, S.; Yamada, K.; Yokomaku, T.; Kamagata, Y.; Kanagawa, T.; Kurane, R. *Anal. Sci.* **2001**, *17*, 155.
(27) (a) Rompaey, E. V.; Sanders, N.; Smedt, S. C.; Demeester, J.; Craenenbroeck, E. V.; Engelborghs, Y. *Macromolecules* **2000**, *33*, 8280. (b) Rompaey, E. V.; Engelborghs, Y.; Sanders, N.; Smedt, S. C.; Demeester, J. *Pharm. Res.* **2001**, *18*, 928. (c) Lucas, B.; Rompaey, E. V.; Smedt, S. C.; Demeester, J.; Oostveldt, P. V. *Macromolecules* **2002**, *35*, 8152. (d) Lucas, B.; Remaut, K.; Braeckmans, K.; Haustraete, J.; Smedt, S. C.; Demeester, J. *Macromolecules* **2004**, *37*, 3832.

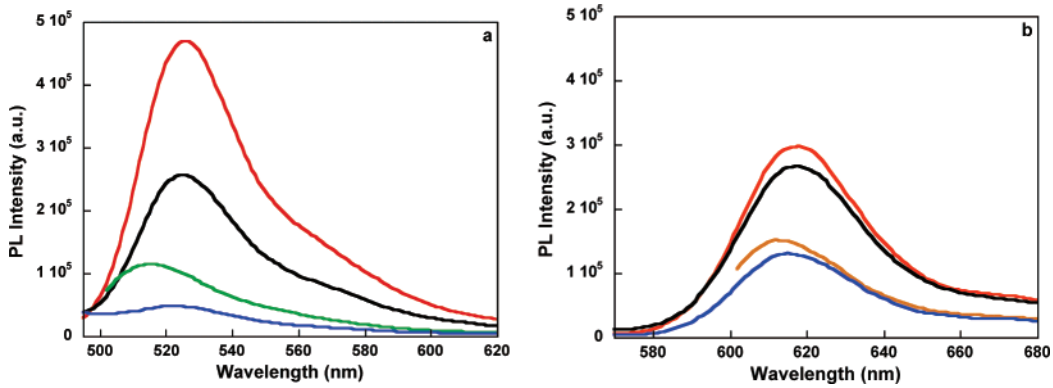

Figure 2. Fluorescence spectra of ssDNA-Fl (a) and ssDNA-TR (b) in the presence of **1** (black), **2** (blue), and **3** (red) in 25 mmol phosphate buffer at [ssDNA-Fl or ssDNA-TR] = 2×10^{-8} M and [RU] = 4×10^{-7} M. The excitation wavelengths are 385 nm for **1** and 365 nm for **2** and **3**. Direct excitation of ssDNA-Fl and ssDNA-TR prior to polymer addition is also shown in green and orange, respectively.

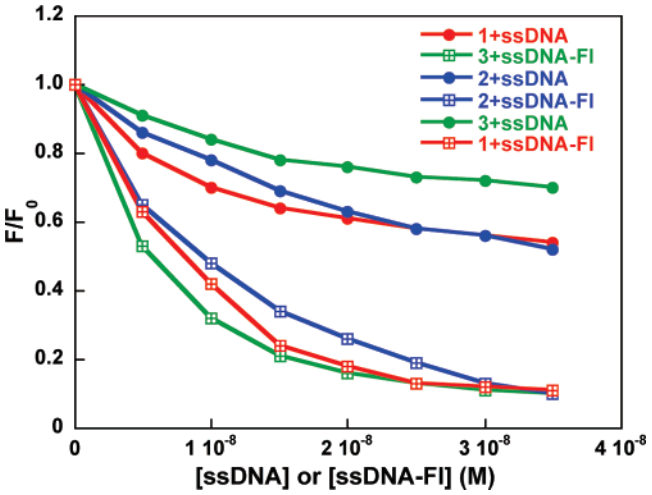

Figure 3. Normalized integrated PL intensity changes in the 390−520 nm range for **1**−**3** ([RU] = 1×10^{-6} M) in the presence of ssDNA or ssDNA-Fl in 25 mM phosphate buffer with the concentration of DNA varying from 0 to 3.5×10^{-8} M (based on strands). F_0 and F are defined as the integrated polymer emission in the absence and in the presence of ssDNA (or ssDNA-Fl), respectively. Excitation wavelength is 385 nm for **1** and 365 nm for **2** and **3**.

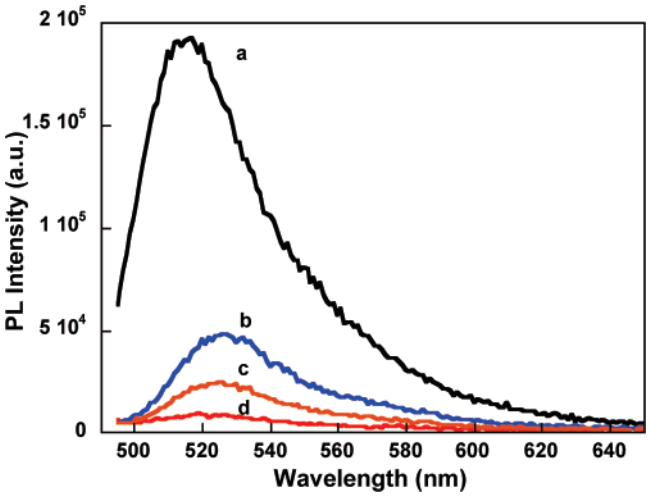

Figure 4. PL spectra of CCP/ssDNA-Fl complexes upon excitation at 495 nm with [ssDNA-Fl] = 2×10^{-8} M and [RU] = 4×10^{-7} M, at $\varphi = 2$: (a) prior to CCP addition and in the presence of (b) **3**, (c) **1**, and (d) **2**.

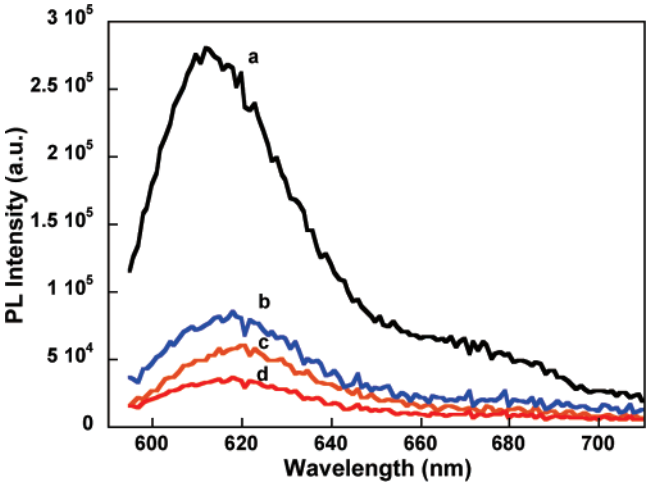

Figure 5. PL spectra of CCP/ssDNA-TR complexes upon excitation at 590 nm with [ssDNA-TR] = 2×10^{-8} M and [RU] = 4×10^{-7} M, at $\varphi = 2$: (a) prior to CCP addition and in the presence of (b) **3**, (c) **1**, and (d) **2**.

complexation were monitored by direct excitation of the dyes at their absorption maxima. These experiments were conducted at [ssDNA-C*] = 2×10^{-8} M, with polymer [RU] varying from 0 to 4×10^{-7} M. Figure 4 compares the Fl PL for **1**/ssDNA-Fl, **2**/ssDNA-Fl, and **3**/ssDNA-Fl at $\varphi = 2$ (φ is the ratio of CCP positive charges relative to ssDNA negative charges), upon direct excitation at 495 nm. An 80% decrease in Fl emission intensity is observed for **1**/ssDNA-Fl and a 90% decrease is observed for **2**/ssDNA-Fl, relative to ssDNA-Fl. Similarly, a 65% decrease takes place with **3**/ssDNA-Fl. Monitoring Fl absorption reveals less than 15% loss upon CCP addition, indicating that the complexes remain in solution and that there is little precipitation or adsorption to surfaces.

Similar experiments to those in Figure 4 were performed using ssDNA-TR instead of ssDNA-Fl. Upon interaction with CCPs, the TR emission is red shifted to 620 nm, relative to free ssDNA-TR (615 nm). TR emission upon direct excitation at its absorption maximum (590 nm) also decreases with increasing [CCP]. Figure 5 compares the TR emission for CCP/ssDNA-TR at $\varphi = 2$, upon direct excitation at 590 nm. Relative to free ssDNA-TR emission, the decreases in emission intensities are 70, 80, and 60% for **1**−**3**, respectively. When one compares the spectra in Figure 5 to those in Figure 4, the intensity loss for TR is only slightly lower than that for Fl.

To probe the possibility of self-quenching, we monitored the Fl emission upon complexation with **1** in ssDNA-Fl/ssDNA mixtures. In these experiments, the ssDNA sequences were

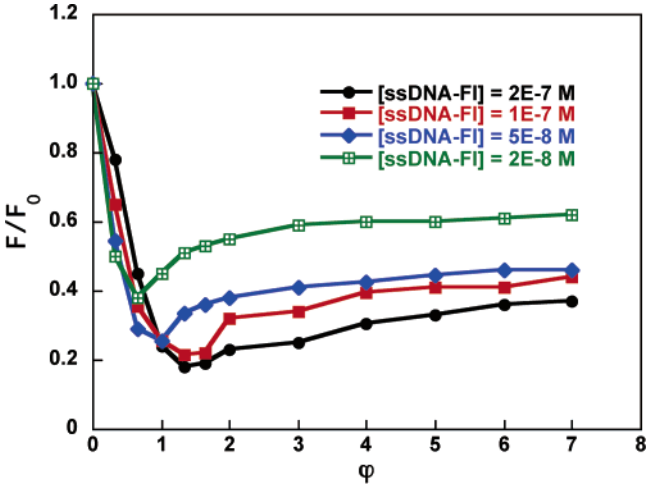

Figure 6. F/F_0 vs φ for **1**/(ssDNA-Fl+ssDNA) complexes with $[ssDNA]_T = 2 \times 10^{-7}$ M, prepared by adding **1** to ssDNA-Fl + ssDNA mixtures. Excitation wavelength is 495 nm.

identical and differed only by the labeling with Fl. Measurements were carried out by adding **1** to solutions with different ratios of ssDNA-Fl and ssDNA, while keeping a constant total $[ssDNA]_T$ = [ssDNA-Fl] + [ssDNA]. F_0 and F values correspond to the emission intensities of Fl in the absence and presence of the CCP, respectively, upon direct excitation, and the ratio F/F_0 provides a measure of the Fl quenching. In the four traces of Figure 6, the ratio of [ssDNA] to [ssDNA-Fl] is varied. The *x*-axis (φ) corresponds to the ± charge ratio. Three important observations can be drawn from Figure 6. First, at all [ssDNA] to [ssDNA-Fl] ratios, the addition of **1** induces a decrease of Fl emission intensity. Second, a higher fraction of ssDNA-Fl in the mixture leads to more pronounced quenching. This observation suggests Fl···Fl self-quenching, which is more pronounced when the local concentration of ssDNA-Fl is highest. Third, the extent of quenching, as indicated by the decrease in F/F_0, reaches its maximum in the $\varphi = 1 \rightarrow 2$ range. Upon further polymer addition, the Fl emission increases. For $\varphi > 2$, one observes a more effective emission recovery when the ssDNA-Fl content in the mixture is lowest. However, even at $\varphi = 7$, the maximum recovery of Fl emission corresponds to approximately 60% of the original PL emission intensity.

The effect of polymer structure on Fl emission quenching was examined as shown in Figure 7. In these experiments, $[ssDNA]_T = 2.0 \times 10^{-7}$ M and [ssDNA-Fl] = 2×10^{-8} M, conditions under which self-quenching is reduced. Different quantities of the CCPs were then added to these solutions, and the decrease in Fl emission, upon direct excitation, was measured. Figure 7 shows that interaction with **2** gives rise to the most efficient quenching with little or no recovery as more polymer is added. More recovery occurs with the addition of **1** or **3**, with **1** being intermediate in terms of net quenching and **3** providing the least perturbation. At $\varphi = 7$, ~25% loss in Fl emission takes place for **3**/ssDNA-Fl + ssDNA, while there is more than 80% loss for **2**/ssDNA-Fl + ssDNA under similar conditions. Examination of the Fl emission in the presence of CCPs reveals a similar shape upon direct excitation or sensitization by the CCPs. Therefore, over 90% of ssDNA-Fl is complexed with the CCPs, and the F/F_0

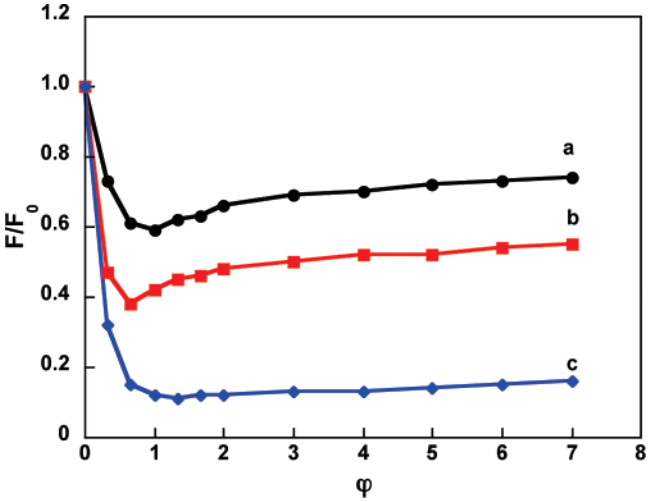

Figure 7. F/F_0 vs φ for CCP/(ssDNA-Fl+ssDNA) solutions prepared by the addition of the CCPs (a for **3**, b for **1**, and c for **2**) to ssDNA-Fl (2×10^{-8} M) + ssDNA (1.8×10^{-7} M) mixtures. Excitation wavelength is 495 nm.

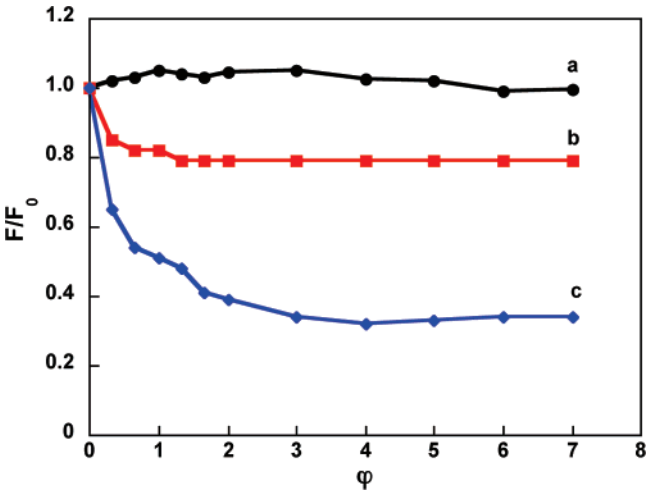

Figure 8. F/F_0 vs φ for CCP/(ssDNA-Fl + ssDNA) solutions prepared by addition CCP (a for **3**, b for **1**, and c for **2**) to ssDNA-TR (2×10^{-8} M) + ssDNA (1.8×10^{-7} M) mixtures. Excitation wavelength is 590 nm.

differences as a function of CCP structures at high φ values are not related to differences in the ratio of free to complexed ssDNA-Fl.

A comparison of TR emission of different CCP/ssDNA-TR mixtures with $[ssDNA]_T = 2 \times 10^{-7}$ M and [ssDNA-TR] = 2×10^{-8} M upon addition of different quantities of **1**−**3** is shown in Figure 8. There is virtually no quenching observed for TR upon interaction with polymer **3** under these conditions, and only ~15% loss of TR emission is observed upon complexation with polymer **1**. When compared to the data in Figure 7, the quenching of acceptor dye emission induced by complexation with the CCPs is less pronounced for TR relative to Fl.

Improved Energy Transfer Conditions. Results from FRET studies between **3** and ssDNA-TR with the TR diluted within the total DNA content ([ssDNA-TR] = 2×10^{-8} M + [ssDNA] = 1.8×10^{-7} M) are shown in Figure 9. Under these conditions, self-quenching of TR is nearly nonexistent. An 18-fold enhancement of the TR emission intensity is observed with [**3**] = 4×10^{-6} M, relative to direct excitation in the absence of **3**. Comparison of these results against the spectra in Figure 2,

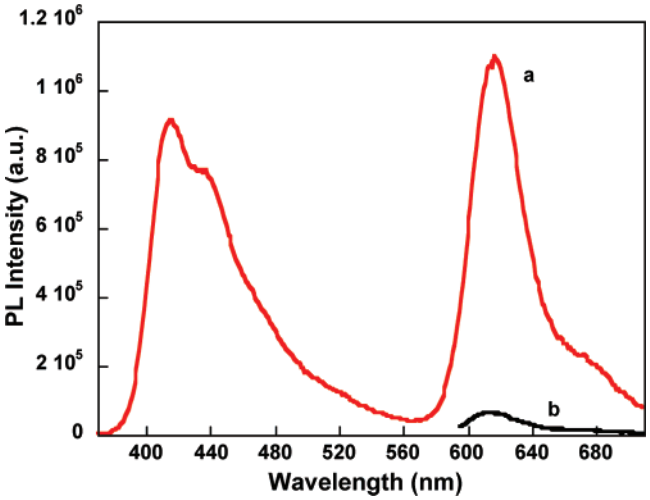

Figure 9. Fluorescence spectra of **3**/ssDNA-TR upon (a) excitation of **3** at 365 nm, (b) direct excitation of TR at 590 nm. Conditions: [ssDNA-TR] = 2×10^{-8} M, [ssDNA] = 1.8×10^{-7} M, [**3**] = 4×10^{-6} M.

where [ssDNA-TR] is similar to that in Figure 9, but only a 2-fold increase in emission is observed, highlights the improved TR emission efficiency in the complex and the impact of TR self-quenching on signal amplification. The net effect of dilution is thus a 9-fold increase in TR emission intensity (upon excitation of **3**).

Discussion

Scheme 3 provides a straightforward access to water-soluble cationic conjugated polymers (CCPs) with fluorene-*co*-phenylene repeat units. Suzuki cross-coupling polymerization of the key intermediate, 2,7-bis[9,9′-(6′′-bromohexyl)-fluorenyl]-4,4,5,5-tetramethyl-[1.3.2]dioxaborolane, with 1,4-dibromo-2,5-substituted phenylene derivatives, affords the neutral CCP precursors. The ionic versions **1**−**3** are produced in 83−89% yields by treatment of the neutral polymers with excess trimethylamine.

While slight differences exist in the absorption maxima of **1**−**3**, their PL spectra, absorption coefficients, and PL quantum yields are very close to each other. Furthermore, the three CCPs have similar rigid backbone structures and molecular weights/polydispersities, and similar transition moment orientations upon interactions with a given acceptor site are expected. Therefore, by taking into account eq 1, one would estimate nearly identical donor capabilities for the three CCPs. However, Figure 2 shows that upon excitation of **1** the emission intensities from Fl and TR are similar, despite the considerably red-shifted absorption band of TR. More striking is that excitation of **2** leads to more intense emission by TR, relative to Fl. Therefore, consideration of eq 1 does not provide a complete picture of the energy transfer processes. Understanding the failure of eq 1 to predict FRET efficiencies and the influence of polymer structure on the emission output of the two acceptors provides the main motivation for subsequent studies.

From the decrease in the CCPs' PL intensities as a function of [ssDNA] provided in Figure 3, one concludes that the three structures show similar levels of self-quenching upon complexation (or aggregation) with ssDNA. The exact sizes, shapes, and orientation of the components in these polyplexes are unknown at this stage but are likely to be dominated by the structural attributes of the polyelectrolyte components, namely, the rigid CCPs and the ssDNA. Additionally, from Figure 3, the three CCPs are quenched to the same extent by ssDNA-Fl. In other words, the chemical nature of the dyes at the terminus of the ssDNA does not appear to influence the general arrangement of the components so that vastly different optical coupling occurs. While there are gaps in our knowledge of the precise arrangement of optical partners in these aggregates, differences in the sensitization of Fl or TR cannot be attributed to different abilities of **1**−**3** to serve as FRET donors.

Direct excitation of the dyes within the CCP and ssDNA-C* mixtures (where C* is either Fl or TR) shows that there is a considerable decrease in the emission efficiency of the dyes, relative to unbound ssDNA-C*. Figures 4 and 5 show the magnitude of this quenching and that the CCP structure plays a role in determining the extent of quenching. From these data, one observes that the degree of quenching matches the dye emission intensity upon CCP excitation, as shown in Figure 2. That is, with **3**, one observes best sensitization of Fl or TR and also the least degree of dye quenching. Similarly, **1** is the intermediate case, in both sensitization and quenching, and **2** gives least energy transfer and most effective quenching. By monitoring the Fl intensity in CCP/ssDNA-Fl + ssDNA mixtures at different φ values and [ssDNA-Fl]/[ssDNA] ratios, as in Figure 6, one observes that the Fl emission recovers at higher CCP/ssDNA ratios ($\varphi > 2$). This recovery is due to diminished dye self-quenching as a result of the dilution within the polyplex structures. Similar quenching behavior of dyes attached to DNA upon condensation with polycations has been observed by using single and dual color fluorescence fluctuation spectroscopies.[27] However, Figure 6 shows that the recovery is not complete, even at high levels of dilution. This latter observation indicates that a fraction of dye quenching by interaction with the CCP is also taking place.

Examination of Fl or TR emission changes (F/F_0) in ssDNA-C*+ssDNA/CCP mixtures, upon direct excitation, as in Figures 7 and 8, leads to the following comments. First, the data further confirm that Fl is more effectively quenched than TR. Second, the quenching of the dye by the CCP under conditions where the dye is diluted with unlabeled ssDNA is dependent on CCP structure. Finding the conditions where dye self-quenching is eliminated is essential for elucidating this CCP/dye quenching phenomenon. Polymer **3** is the least effective quencher. By using **3** and taking into account that dye self-quenching can be reduced by "diluting" ssDNA-TR with unlabeled DNA, it is possible to find conditions where there is no quenching of TR emission, relative to free ssDNA-TR. A similar success could not be achieved with ssDNA-Fl.

Our efforts to understand how the polymer molecular structure influences the optical performance of the dyes within the polyplex structures begin by examination of the molecular orbital energy levels of the optical partners and the background provided in Scheme 1. The HOMO and LUMO energy levels of the different molecular components were estimated using cyclic voltammetry and absorption spectroscopy and are listed in Table 2. Although we do not have the cyclic voltammetry data of CCPs in water, the neutral precursors allow a relative comparison of donor/acceptor orbital energy levels. Additionally recent studies have shown that there is negligible difference in the HOMO and LUMO levels of a neutral precursor and a

charged counterpart in the solid state.[28] The difference in oxidation and reduction potentials between the neutral polymers in THF and the CCPs in water is thus estimated to be ±0.1 V, assuming that there is no coupled electron and proton transfer between the CCPs and water.[29]

From Table 2 we note that CCP HOMO and LUMO energies track the expected trend based on the electron releasing/withdrawing properties of the substituents on the phenylene comonomer.[20d] Fluorine substitution lowers the energy levels, while the electron donating methoxy group raises the levels, relative to the unsubstituted parent structure **1**. The Fl LUMO energy (−3.6 eV) is contained within the HOMO−LUMO gap of the three polymers. However, the Fl HOMO energy (−5.9 eV) is lower than those of polymers **1** (−5.6 eV) and **2** (−5.4 eV). For these two structures it is reasonable to expect that situation B in Scheme 1, i.e. PCT to the LUMO of Fl, is taking place. For polymer **3**, with a HOMO energy of −5.8 eV, the situation is less clear and given the limitations of Scheme 1 both processes may be taking place to some extent. We point out that there is ± 0.3 eV uncertainty on the average energy level values and that a range of energy levels can be expected in a sample, given the molecular weight distributions and ranges of environment within the polyplex structures, i.e., interchain delocalization.[30] Despite these uncertainties, it is evident that electron withdrawing substituents allow the Fl HOMO to be better contained within the HOMO−LUMO gap of the π-conjugated system and give rise to a reduced driving force for charge transfer. Indeed, this is the situation observed experimentally. Excitation of polymer **3** provides the highest Fl emission intensity, while polymer **2** is the least effective in this respect.[31]

The TR HOMO level (−5.4 eV) is higher than those of **1** and **3** and is close in energy to the level of **2** (Table 1). In fact, the HOMO−LUMO levels of TR are well contained between the levels of **3**, as in situation A in Scheme 1 which should favor FRET over PCT. Additionally, that the energy gap between TR and the three CPs is greater than that observed with Fl should provide additional driving force for energy transfer, relative to charge transfer.[14c]

Direct dye excitation experiments provide complementary information to the FRET experiments. That the Fl PL quantum efficiency is considerably reduced (Figures 4 and 7), is consistent with the analysis of orbital energies provided above and with the possibility of PCT quenching, by hole transfer to the CCP HOMO.[13] Direct excitation of TR in CCP/ssDNA-TR polyplexes shows that the quenching is much less severe than for Fl (Figures 5 and 8). When one examines the PL output of TR when in the presence of polymer **3** under conditions where no TR---TR self-quenching is operative, it is possible to unambiguously rule out PCT.

Mechanistic insight can be applied to optimize solutions of **3** with ssDNA-TR so that an 18-fold signal amplification in the TR emission can be obtained by FRET from **3**, despite poor spectral overlap. In the absence of TR dilution, only a 2-fold enhancement is observed. The degree of enhancement is considerably lower with **1** or **2**, primarily because of the underlying quenching of the dye emission by the polymers.

Conclusion

An improved access to cationic conjugated polymers (CCPs) with fluorene-phenylene repeat units containing substituents that modulate the electron density in the polymer backbone has been developed. These materials were used to dissect the efficiency of energy transfer to dye labeled DNA. We found that the three CCPs under study are quenched to similar extent by Fl or TR. For both dyes, we found that there is considerable self-quenching upon complexation with the CCPs. This self-quenching can be minimized upon "dilution" of ssDNA-C* with unlabeled ss-DNA. The efficiencies of dye emission are more significantly affected by the interactions with the CCPs, with Fl being more effectively quenched than TR. Reduction of electron density on the polymer backbone through substitution with electron withdrawing fluorine leads to a reduction of the quenching process. Examination of the molecular orbital energies determined by electrochemical and optical techniques and correlation against the dependence of FRET and PCT on the relative ordering of donor and acceptor orbital energies provides for a possible rationale of the results. Taking into account these mechanistic considerations, it is possible to optimize the emission of the reporter dye by reducing the total fraction of DNA that is labeled with the reporter dye. Furthermore, it is interesting to note that much of the previous sensitivities of CCP sensors that operate by energy transfer to Fl-labeled bimolecular probes can be considerably improved by utilizing less electronegative dyes.

Experimental Procedures

General Details. ^{1}H and ^{13}C NMR spectra were collected on a Varian ASM-100 200 MHz spectrometer. The UV−Vis absorption spectra were recorded on a Shimadzu UV-2401 PC diode array spectrometer. Fluorescence was measured using a PTI (Lawrenceville, NJ) Quantum Master fluorometer equipped with a xenon lamp excitation source and a Hamamatsu (Japan) 928 PMT, using 90 degree angle detection for solution samples. HPLC purified DNA oligonucleotides were obtained from Sigma Genosys and the concentrations were determined using 260 nm absorbance measurements in 200 μL quartz cells in a Beckman (Fullerton, CA) DU800 spectrophotometer. All the reagents and chemicals were obtained from Aldrich Co. and were used as received. 2,7-dibromo-9,9-bis(6′-bromohexyl)fluorene was synthesized according to the reported procedure.[16b]

Synthesis. 2,7-bis[9,9′-bis(6″-bromohexyl)-fluorenyl]-4,4,5,5-tetramethyl-[1.3.2]dioxaborolan e. A 50 mL round-bottom flask was charged with 9,9′-bis(6′-bromohexyl)-2,7-dibromofluorene (0.65 g, 1 mmol) in 20 mL of dry THF and cooled to −78 °C with a dry ice/acetone bath. At −78 °C, 2.5 eq. of *t*-BuLi in pentane (1.8 mL, 1.7 M) was added drop by drop and the mixture was stirred for an hour. It was followed immediately by adding 2-isopropoxy-4,4,5,5-tetramethyl-[1.3.2]-dioxaborolane (1.3 mL, 6 mol) in one shot. The resulting solution was kept at −78 °C for additional 2 h. The resulting mixture was quenched by water, and the solution was concentrated by rotary evap-

(28) Huang, F.; Wu, H.; Wang, D.; Yang, W.; Cao, Y. *Chem. Mater.* **2004**, *16*, 708.
(29) Seidel, C. A.; Schulz, M.; Sauer, H. *J. Phys. Chem.* **1996**, *100*, 5541.
(30) (a) Gebhardt, V.; Bacher, A.; Thelakkat, M.; Stalmach, U.; Meier, H.; Schmidt, H. W.; Haarer, D. *Adv. Mater.* **1999**, *11*, 119. (b) Chang, R.; Hsu, J. H.; Fann, W. S.; Liang, K. K.; Chang, C. H.; Hayashi, M.; Yu, J.; Lin, S. H.; Chang, E. C.; Chuang, K. R.; Chen, S. A. *Chem. Phys. Lett.* **2000**, *317*, 142.
(31) We reemphasize here that the framework we provide for understanding the level of quenching of the dye by the different CCP structures is based on the thermodynamic driving force for PCT. Possible kinetic differences based on the acceleration of charge transfer with increasing driving force within the normal region, as described by Marcus, are not included and may bear an important contribution to the different levels of quenching. See: (a) Creutz, C.; Keller, A. D.; Sutin, N.; Zipp, A. P. *J. Am. Chem. Soc.* **1982**, *104*, 3618. (b) Dossot, M.; Allonas, X.; Jacques, P. *Phys. Chem. Chem. Phys.* **2002**, *4*, 2989. (c) Sim, E. *J. Phys. Chem. B* **2005**, *109*, 11829 and ref 14b.

oration and extracted with chloroform. The organic phase was separated and dried over magnesium sulfate. After evaporation, the reside was purified with silica gel column chromatography (CH_2Cl_2/hexane 1:3) to yield 0.32 g (42%) of the product as white crystals. ^{1}H NMR (400 MHz, $CDCl_3$): δ 7.83−7.72 (m, 6H), 3.27−3.24 (t, J = 6.8 Hz, 4H), 2.03−1.99 (q, J = 4.0 Hz, 4H), 1.64−1.57 (q, J = 7.2 Hz, 4H), 1.39 (s, 24 H), 1.17−1.13 (q, 4H), 1.06−1.02 (q, 4H), 0.55 (m, 4H). ^{13}C NMR (100 MHz, $CDCl_3$): δ 150.27, 144.09, 133.99, 128.93, 119.67, 83.97, 55.24, 40.12, 34.19, 32.84, 29.15, 27.93, 23.55. MS(EI) *m*/*z* 744 (M^+).

Poly(9,9′-bis(6′′-bromohexyl)fluorene-*co*-*alt*-1,4-phenylene) (**1a**). 2,7-Dibromo-9,9′-bis(6′′-bromohexyl)fluorene (325 mg, 0.5 mmol), 1,4-phenyldiboronic acid (82.9 mg, 0.5 mmol), Pd(dppf)Cl_2 (7 mg) and potassium carbonate (830 mg, 6 mmol) were placed in a 25 mL round-bottom flask. A mixture of water (3 mL) and THF (6 mL) was added to the flask and the reaction vessel was degassed. The mixture was refluxed at 85 °C for 24 h, and then precipitated into methanol. The polymer was filtered and washed with methanol and acetone, and then dried under vacuum for 24 h to afford 1a (220 mg, 78%), as an off-white solid. ^{1}H NMR (200 MHz, $CDCl_3$): δ 7.8−7.5 (m, 10H), 3.3 (t, 4H), 2.1 (m, 4H), 1.7 (m, 4H), 1.3−1.2 (m, 8H), 0.8 (m, 4H). ^{13}C NMR (50 MHz, $CDCl_3$): δ 151.9, 140.9, 140.7, 140.2, 128.1, 126.6, 121.8, 120.8, 55.7, 40.9, 34.5, 33.2, 29.6, 28.3, 24.2.

Poly(9,9′-bis(6′′-bromohexyl)fluorene-*co*-*alt*-2,5-dimethoxy-1,4-phenylene) (**2a**). 2,7-Bis[9,9′-bis(6′′-bromohexyl)-fluorenyl]-4,4,5,5-tetramethyl-[1.3.2]dioxabor olane (372 mg, 0.5 mmol), 1,4-dibromo-2,5-dimethoxybenzene (148 mg, 0.5 mmol), Pd(PPh_3)$_4$ (5 mg) and potassium carbonate (830 mg, 6 mmol) were placed in a 25 mL round-bottom flask. A mixture of water (3 mL) and toluene (5 mL) was added to the flask and the reaction vessel was degassed. The mixture was vigorously stirred at 85 °C for 24 h and then precipitated into methanol. The polymer was filtered and washed with methanol and acetone, and then dried under vacuum for 24 h to afford **2a** (240 mg, 76%), as white fibers. ^{1}H NMR (200 MHz, $CDCl_3$): δ 7.8−7.1(m, 8H), 3.8 (s, 6H), 3.3−3.2 (t, 4H), 2.1 (m, 4H), 1.7 (m, 4H), 1.3−1.2 (m, 8H), 0.9 (m, 4H). ^{13}C NMR (50 MHz, $CDCl_3$): δ 151.3, 150.7, 140.2, 137.2, 132.4, 128.3, 124.7, 119.7, 115.7, 57.2, 55.2, 40.4, 34.2, 33.0, 29.5, 28.1, 24.2.

Poly(9,9′-bis(6′′-bromohexyl)fluorene-*co*-*alt*-2,5-difluoro-1,4-phenylene) (**3a**). 2,7-Bis[9,9′-bis(6′′-bromohexyl)-fluorenyl]-4,4,5,5-tetramethyl-[1.3.2]dioxabor olane (372 mg, 0.5 mmol), 1,4-dibromo-2,5-difluorobenzene (136 mg, 0.5 mmol), Pd(PPh_3)$_4$ (5 mg) and potassium carbonate (830 mg, 6 mmol) were placed in a 25 mL round-bottom flask. A mixture of water (3 mL) and toluene (5 mL) was added to the flask and the reaction vessel was degassed. The mixture was vigorously stirred at 85 °C for 24 h, and then precipitated into methanol. The polymer was filtered and washed with methanol and acetone, and then dried under vacuum for 24 h to afford **3a** (221 mg, 73%), as white fibers. ^{1}H NMR (200 MHz, $CDCl_3$): δ 7.8−7.2 (m, 8H), 3.3−3.2 (t, 4H), 2.1 (m, 4H), 1.7 (m, 4H), 1.3−1.2 (m, 8H), 0.9 (m, 4H). ^{13}C NMR (50 MHz, $CDCl_3$): δ 158.4, 153.6, 151.3, 140.7, 133.8, 128.1, 123.6, 120.5, 118.1, 55.2, 40.3, 34.2, 32.8, 29.2, 27.9, 23.8.

Poly[(9,9′-bis(6′′-(*N*,*N*,*N*,-trimethylammonium)-hexyl)fluorene-*co*-*alt*-1,4-phenylene) dibromide] (**1**). Condensed trimethylamine (2 mL) was added dropwise to a solution of the neutral polymer **1a** (60 mg) in THF (10 mL) at −78 °C. The mixture was allowed to warm to room temperature. The precipitate was redissolved by the addition of water (10 mL). After the mixture was cooled to −78 °C, extra trimethylamine (2 mL) was added and the mixture was stirred for 24 h at room temperature. After removing most of the solvent, acetone was added to precipitate **1** (72 mg, 89%) as an off-white powder. ^{1}H NMR (200 MHz, CD_3OD): δ 8.0−7.8 (m, 10H), 3.3−3.2 (t, 4H), 3.1 (s, 18H), 2.3 (br, 4H), 1.6 (br, 4H), 1.3 (br, 8H), 0.8 (br, 4H). ^{13}C NMR (50 MHz, CD_3OD): δ 151.8, 140.9, 140.4, 140.0, 127.6, 126.1, 121.2, 120.5, 66.7, 55.7, 52.5, 40.2, 29.2, 25.8, 23.7, 22.5.

Poly[9,9′-bis(6′′-*N*,*N*,*N*-trimethylammonium)-hexyl)fluorene-*co*-*alt*-2,5-dimethoxy-1,4 phenylene) dibromide] (**2**). Condensed trimethylamine (2 mL) was added dropwise to a solution of the neutral polymer **2a** (70 mg) in THF (10 mL) at −78 °C. The mixture was allowed to warm to room temperature. The precipitate was redissolved by the addition of water (10 mL). After the mixture was cooled to −78 °C, extra trimethylamine (2 mL) was added and the mixture was stirred for 24 h at room temperature. After removing most of the solvent, acetone was added to precipitate **2** (80 mg, 83%) as an off-white powder. ^{1}H NMR (200 MHz, CD_3OD): δ 7.8−7.6 (m, 8H), 3.9 (s, 2H), 3.3−3.2 (m, 4H), 3.1 (s, 18H), 2.2 (br, 4H), 1.6 (br, 4H), 1.3 (br, 8H), 0.8 (br, 4H). ^{13}C NMR (50 MHz, CD_3OD): δ 152.5, 151.7, 141.6, 138.7, 132.3, 129.6, 126.3, 120.8, 116.5, 67.8, 57.6, 56.4, 53.6, 31.0, 30.5, 27.0, 25.0, 23.7.

Poly[9,9′-bis(6′′-*N*,*N*,*N*-trimethylammonium)-hexyl)fluorene-*co*-*alt*-2,5-difluoro-1,4-phenylene) dibromide] (**3**). Condensed trimethylamine (2 mL) was added dropwise to a solution of the neutral polymer **3a** (60 mg) in THF (10 mL) at −78 °C. The mixture was allowed to warm to room temperature. The precipitate was redissolved by the addition of water (10 mL). After the mixture was cooled to −78 °C, extra trimethylamine (2 mL) was added and the mixture was stirred for 24 h at room temperature. After removing most of the solvent, acetone was added to precipitate **3** (74 mg, 84%) as a white powder. ^{1}H NMR (200 MHz, CD_3OD): δ 7.8−7.5 (m, 8H), 3.3−3.2 (m, 4H), 3.1 (s, 18H), 2.2 (br, 4H), 1.6 (br, 4H), 1.3 (br, 8H), 0.8 (br, 4H). ^{13}C NMR (50 MHz, CD_3OD): δ 159.8, 151.7, 154.9, 152.6, 142.4, 135.1, 129.4, 124.8, 121.6, 119.2, 67.8, 53.5, 50.4, 41.2, 31.0, 30.5, 27.1, 23.7.

Acknowledgment. This work was supported by a National Institute of Health Grant (GM 62958-01), the NSF (DMR-0097611), and the Institute for Collaborative Biotechnologies.

JA055382T